

Chapter 3

Simulation

3.1 Introduction

Our module, including fiberlens, mirror and SIL, was proposed in the previous chapter, as shown in Fig.3-1. In this chapter, all components were designed and the tolerances of this module were analyzed.

First, an optical model of this module was established. The mirror was ignored in the optical module because it was only used to redirect the beam. Then the dimensions of all components were optimized under the criteria of optical quality and fabrication limitations. Fiberlens length, distance between fiberlens and SIL and the dimension of SIL were the variables to be considered. Finally, system tolerances were analyzed according to the optical quality degradation caused from fabrication errors and integration misalignments, including: axial, lateral and angular. More detailed descriptions about our module design are described in next section.

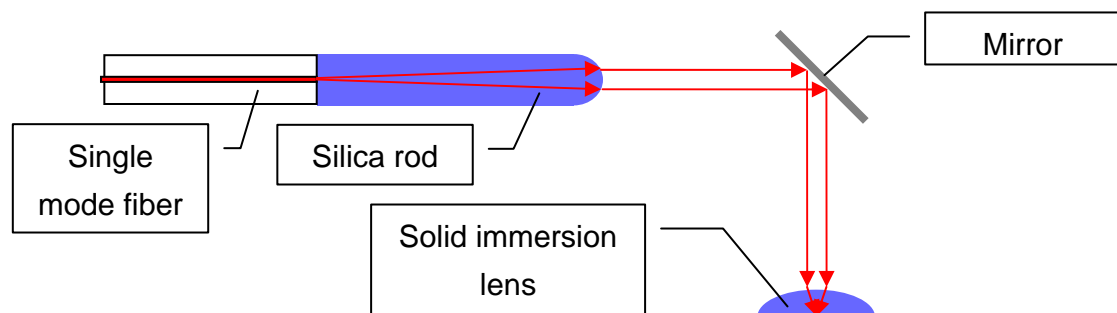


Fig. 3-1 Planar fiber-base pickup head setup

3.2 Optimizing Process

The DVD specification requires $NA=0.6$, wavelength= $650 \mu\text{m}$ and spot size = $1.1 \mu\text{m}$. We expect our module have a better performance than DVD specification so the criteria of optical quality are as follows: the output beam size which is defined as full-width at $1/e^2$ maximum intensity is less than $1 \mu\text{m}$; total NA is larger than 0.6; the process window is within the system tolerance. The limitations of fabrication are determined by resolution of the machines. In MOEMS technology, the limitation is about $1 \mu\text{m}$. The optical module is given in Fig.3-2.

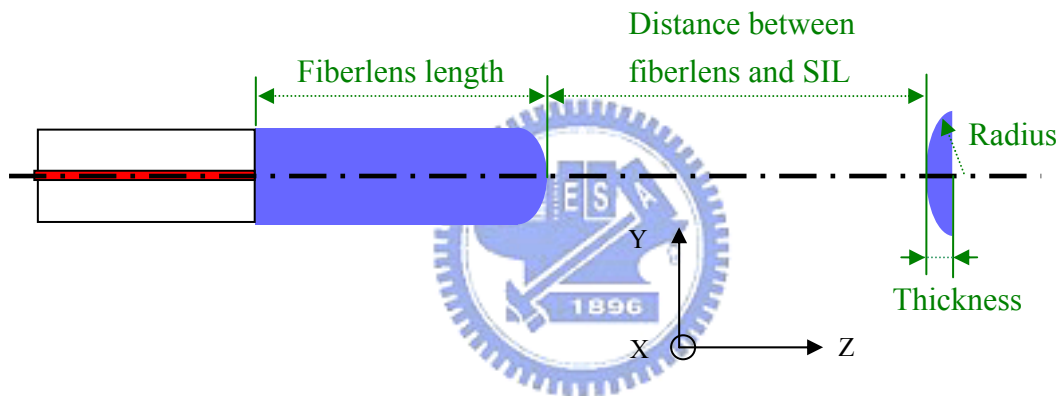


Fig. 3-2 Schematics of optical module

The fiber is used to guide laser beam into the module set as the laser source of $4.3 \mu\text{m}$ beam width. The fiberlens is used as objective lens to focus laser beam. The relation between the output beam quality and fiberlens is simulated. The optimized value of fiberlens is got by the criteria of optical quality. The output field is used as the incident beam of solid immersion lens.

Next, we consider two kinds of the perfect SIL, hemispherical SIL and SSIL. The thickness of SIL has a linear relation with the radius so they are the same variable. According to the optical quality of output beam which passes through fiberlens and SIL, the thickness is optimized. The fiberlens also needs to be modified to achieve our

target which is better than DVD specification. After iteration process, the system parameter is decided.

Because actually the fiberlens and SIL have some errors in fabrication and in assembly process, the misalignment is considered and the tolerance of this module is simulated.

Finally, the feasibility of this module can be verified by comparing the tolerance with fabrication window. The optimizing process is show in Fig.3-3.

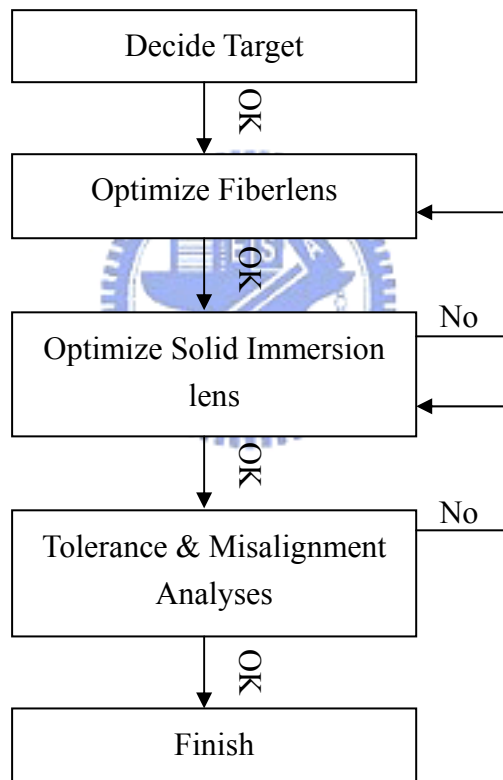


Fig. 3-3 Optimizing process flow

3.2.1 Fiberlens

The fiberlens is used as objective lens to focus laser beam. The relation between the output beam quality and fiberlens length is obtained according to the fundamental

theory, paraxial Gaussian beam (ABCD). The design of fiberlens is restricted by the dimensions limitation of fiberlens, the basic theory of SIL and the target of our module, spot size $< 1 \mu\text{m}$ and $\text{NA} > 0.6$.

Because the shape of fiberlens is formed by cohesion, the radius of curvature of fiberlens is assumed $62.5 \mu\text{m}$ which is equal to the radius of single mode fiber, the minimum radius of fiberlens can be made. The fiberlens simulation model is given in **Fig.3-4**. Spot size is defined as the minimum beam width in focal plane. As fiberlens length is larger than $820 \mu\text{m}$, total reflection occurs at the convex surface, as shown in **Fig.3-5**, so the maximum fiberlens length is $820 \mu\text{m}$. **Fig.3-6** shows fiberlens length versus NA and spot size. The NA is in linear relation with fiberlens length. The spot size is similar to exponential decay.

Two kinds of SIL, hemispherical SIL and SSIL are discussed in our simulation. In hemispherical SIL, the spot size of fiberlens is computed by using the equation **(2-10a)** where the refractive index of SIL is 1.8. According to the criterion of final spot size being less than $1 \mu\text{m}$, the spot size of fiberlens should be less than $1.8 \mu\text{m}$, while the correspondent fiberlens length is at least $650 \mu\text{m}$ and NA is 0.21 from **Fig.3-6**. According to the criterion of effective NA being larger than 0.6, the fiberlens NA should be larger than 0.3333 using the equation **(2-10b)**. From the **Fig.3-6**, the fiberlens is at least $920 \mu\text{m}$ and the spot size is as small as $1.2 \mu\text{m}$. From the result above, fiberlens length of at least $920 \mu\text{m}$ can meet both the criteria. However, $920 \mu\text{m}$ is larger than maximum fiberlens length, $820 \mu\text{m}$. Therefore, the NA and spot size can't achieve the target while using hemispherical SIL. The NA is 0.286 and The spot size is $1.3 \mu\text{m}$ as the fiberlens length is $820 \mu\text{m}$. Although this can't meet the requirement, fiberlens length of $820 \mu\text{m}$ still can be used to proof the simulation result because hemispherical SIL is easier to fabricate.

In Super SIL (SSIL), the spot size of fiberlens is computed by using the equation

(2-11a) where the refractive index of SIL is 1.8. According to the criterion of final spot size being less than $1 \mu\text{m}$, the spot size of fiberlens should be less than $3.24 \mu\text{m}$, while the corresponding fiberlens length is of at least $450 \mu\text{m}$ and NA is larger than 0.12 from Fig.3-6. According to the criterion of effective NA being larger than 0.6, the fiberlens NA should be larger than 0.185 using the equation (2-11b). From Fig.3-6, the fiberlens is at least $564 \mu\text{m}$ and the spot size is as small as $2.6 \mu\text{m}$. From the result above, fiberlens length of at least $564 \mu\text{m}$ can meet both the criteria.

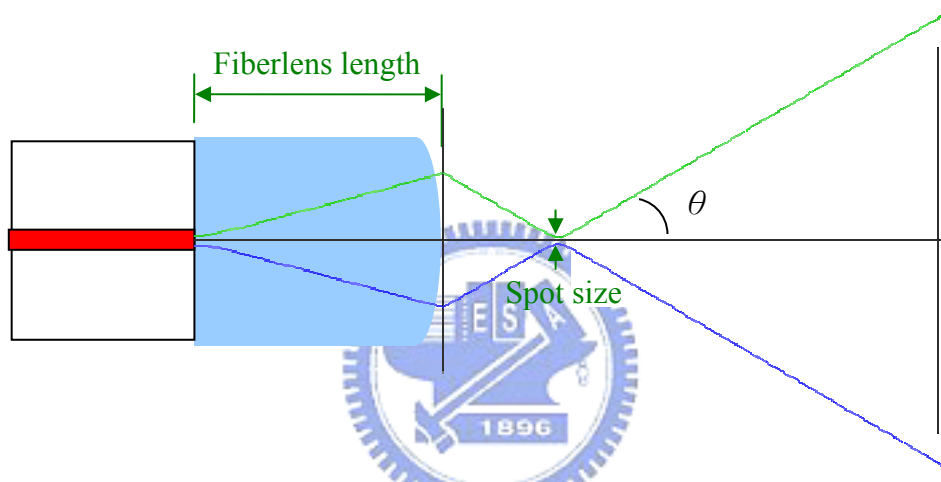


Fig. 3-4 Fiberlens setup

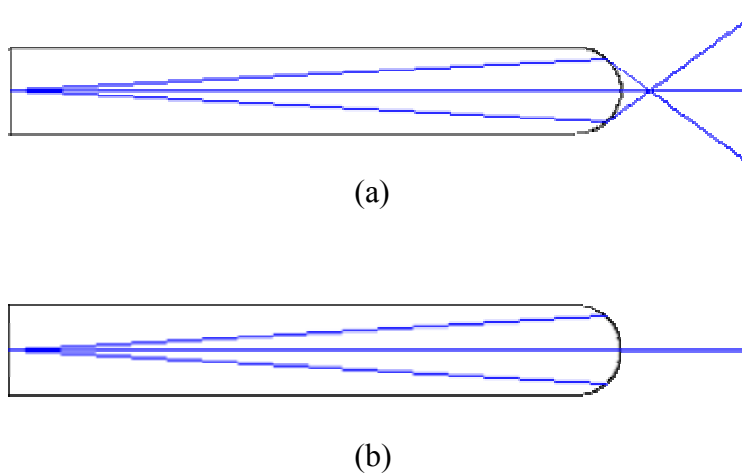


Fig. 3-5 (a) Normal (b) Total reflection

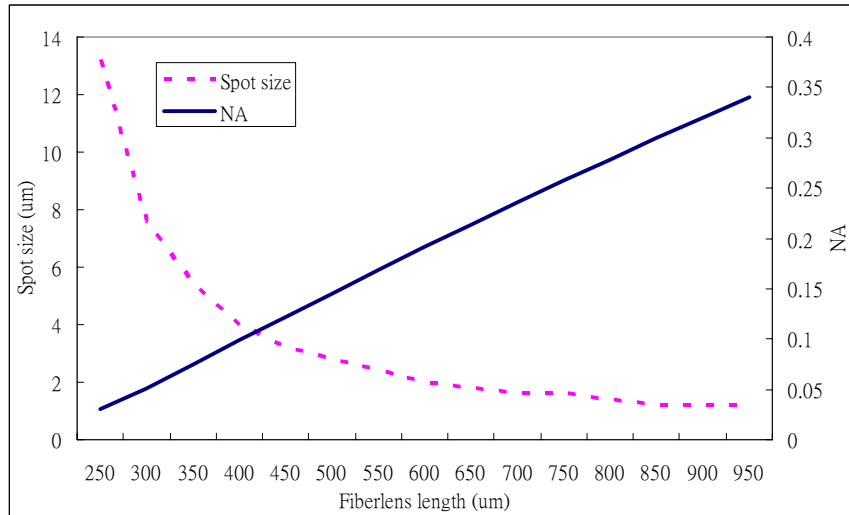


Fig. 3-6 Fiberlens length vs. Spot size and NA

3.2.2 Fiberlens & Solid Immersion Lens

The SIL is used to further reduce the spot size by increasing the effective NA. The target spot size at the bottom side of SIL was set under $1 \mu\text{m}$, while the incident spot size was $1.3 \mu\text{m}$ in hemispherical SIL and $2.6 \mu\text{m}$ in SSIL mentioned in the previous section, respectively. The effective NA was set to be 0.6, while the incident NAs were 0.286 in hemispherical SIL and 0.185 in SSIL, respectively.

The criteria come from the refractive index and two types of SIL. SIL is made from AZ4620 whose the refractive is 1.8. Two kinds of SIL, hemispherical SIL and SSIL, were considered in our design, as show in Fig.3-7. The thickness and radius are set to be r in hemispherical SIL. The radius has relation with thickness in SSIL as follows:

$$thickness = radius \times \left(1 + \frac{radius}{n}\right) \quad (3-1)$$

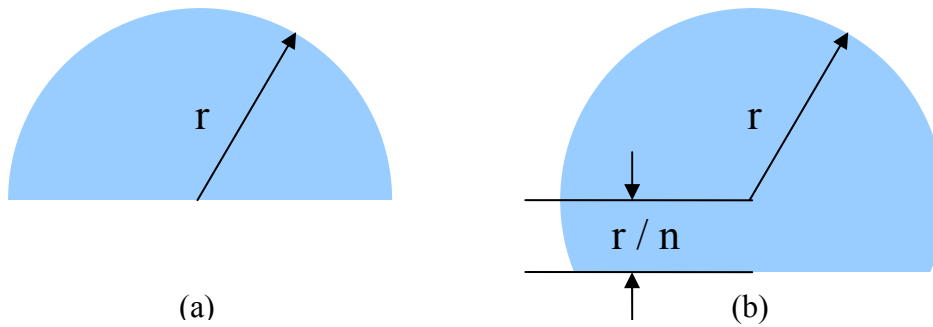


Fig. 3-7 (a) hemispherical SIL and (b) SSIL

The parameter to be considered is thickness of SIL. SIL is fabricated by Micro Optics Electro Mechanical System (MOEMS) technology, so it has two limitations: the minimum thickness is about $10 \mu\text{m}$ and the maximum thickness is $33 \mu\text{m}$ because of the coating process and absorption issue. As the thickness becomes thicker, the absorption increases. Fig.3-8 shows the relation between the absorption and thickness of AZ4620 at 633nm [1]. The beam intensity after pass through the resist (I_f) is determined by the intensity incident on the glass slide (I_o). The absorption is defined as $\ln(I_o / I_f)$. The maximum transmission is required to be at least over 50%, while the absorption is equal to 0.7. Therefore, the thickness of SIL is restricted to be less than $33 \mu\text{m}$.

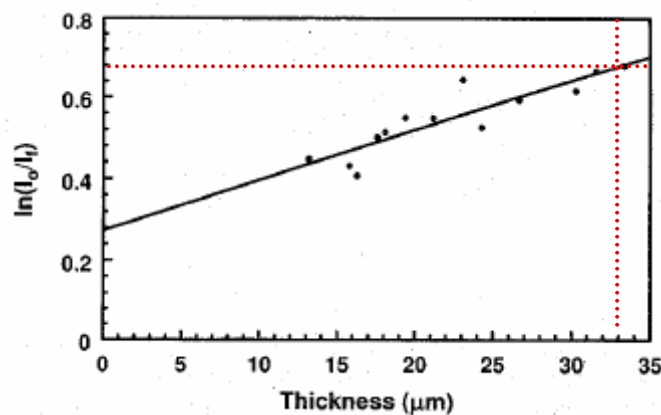


Fig. 3-8 Absorption versus thickness of the AZ-4620 (C. R. King et al., 1996)

The paraxial Gaussian beam (ABCD) law is used to optimize SIL. The simulation model of fiberlens and SIL is given in Fig.3-9. The optimized fiberlens length from the previous result is set as the input condition. The distance between fiberlens and SIL is precisely controlled to ensure that minimum beam width is located at the bottom of SIL. The beam emitted from fiber passes through fiberlens and SIL into air. The final spot size is defined as the beam width at the bottom of SIL. The effective NA is computed from $\sin \theta$ which is the angle of output beam far from focal plane.

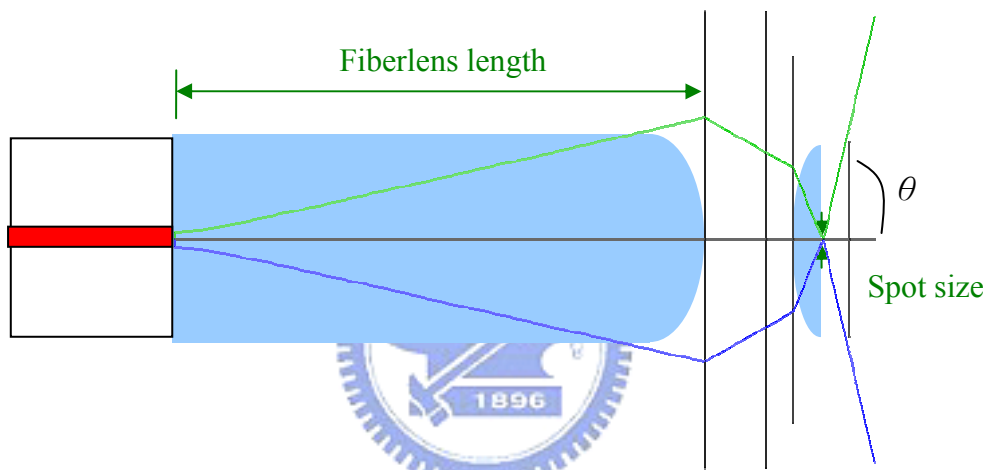


Fig. 3-9 Fiberlens and SIL setup

For hemispherical SIL, $820 \mu\text{m}$ fiberlens is used and the thickness is adjusted from $10 \mu\text{m}$ to $34 \mu\text{m}$. Fig.3-10 shows the relation between beam quality and thickness of SIL. The thickness almost doesn't have any effect. The spot size is $0.776 \mu\text{m}$ which is close to $0.722 \mu\text{m}$ from equation (2-10a) where the spot size of $820 \mu\text{m}$ fiberlens is $1.3 \mu\text{m}$. The effective NA is about 0.48 which is close to 0.51 from equation (2-10b) where the NA of $820 \mu\text{m}$ fiberlens is 0.285. By considering the absorption, the thickness should be as small as possible. In contrast, the thickness should be as large as possible for convenience of alignment during assembly process. We choose the thickness of SIL is $25 \mu\text{m}$ in order to increase the tolerance of alignment.

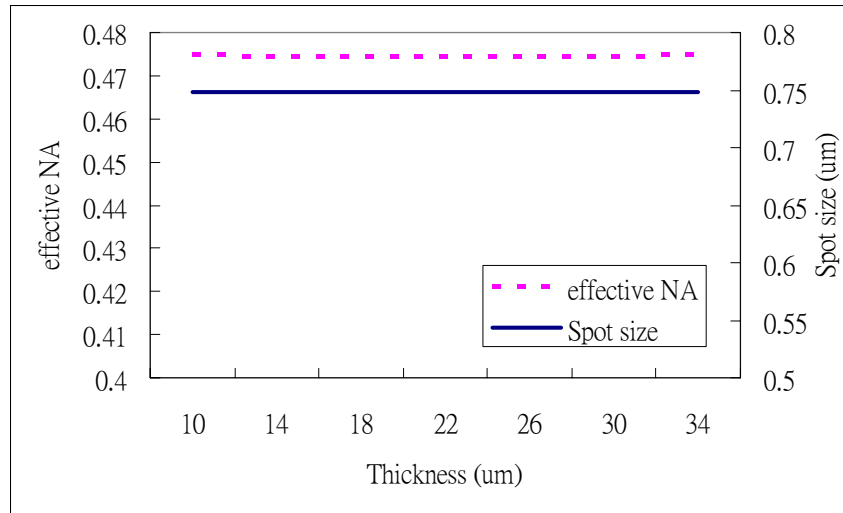


Fig. 3-10 Thickness of hemispherical SIL vs. effective NA & Spot size

In SSIL, the optimized fiberlens length is $564 \mu\text{m}$ and the thickness is adjusted from $10 \mu\text{m}$ to $33 \mu\text{m}$. The relation between beam quality and thickness of SIL is shown in Fig.3-11. The thickness still has no effect. The spot size is about $0.7 \mu\text{m}$ which is close to $0.71 \mu\text{m}$ from equation (2-11a) where the spot size of $564 \mu\text{m}$ fiberlens is $2.3 \mu\text{m}$. The effective NA is about 0.49 which is far from 0.6 from equation (2-11b) where the NA of $564 \mu\text{m}$ fiberlens is 0.185. It is far below the target because equation (2-11b) is an approximation. Obviously, the fiberlens length should be increased to meet the requirement. Due to the ratio of effective NA, say 0.49, to the NA of fiberlens, 0.185, is about 2.64, the NA of fiberlens is estimated about 0.235 when the effective NA is assumed 0.6. From Fig.3-6, the fiberlens length is about $700 \mu\text{m}$ when the fiberlens NA is about 0.235.

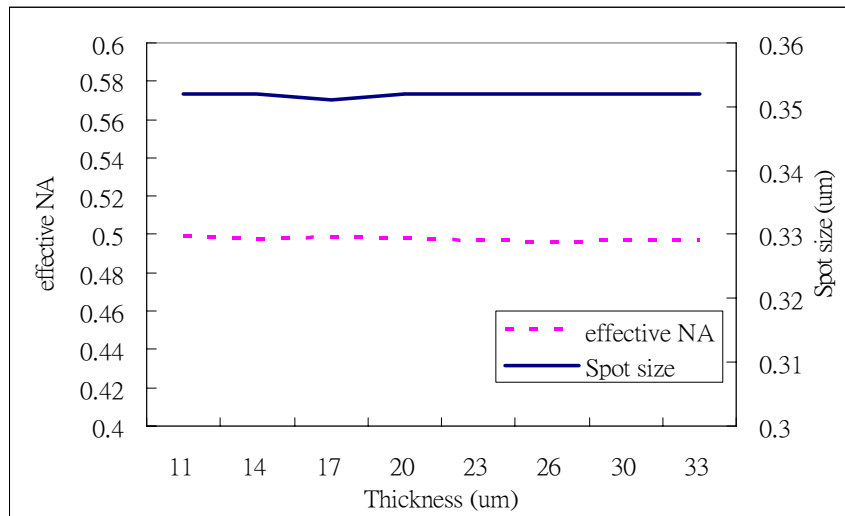


Fig. 3-11 Thickness of SSIL vs. effective NA & Spot size @ 564um fiberlens

When the fiberlens length is $700 \mu\text{m}$, the relation between beam quality and thickness of SIL is shown in Fig.3-12. The spot size is about $0.51 \mu\text{m}$ which is of less than our target, $1 \mu\text{m}$. The NA is about 0.61 which is close to 0.6 , our requirement. We choose the thickness of SIL is $23 \mu\text{m}$ in order to increase the easeness of alignment. Since the optimized system has been designed, the system tolerance in fabrication and misalignment in assembly process will be discussed in the following section.

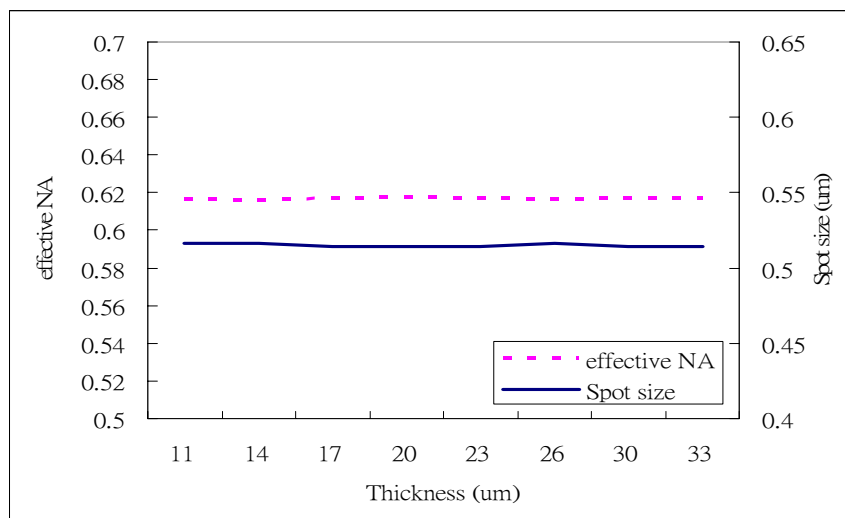


Fig. 3-12 Thickness of SSIL vs. effective NA & Spot size @ 700um fiberlens

3.3 Dimension & Alignment tolerance analyses

According to the simulation, the module has been designed and optimized in idea case. A spot which is less than $1 \mu\text{m}$ was obtained at the bottom of SIL and the effective NA was larger than 0.6. However, the optical signal degradation occurs due to the errors from fabrication, radius of fiberlens and thickness of SIL, assembly process, offset, and tilt. Therefore, the optical system tolerances correspond to radius of fiberlens and thickness of SIL was analyzed based on the fabrication process and output beam criteria.

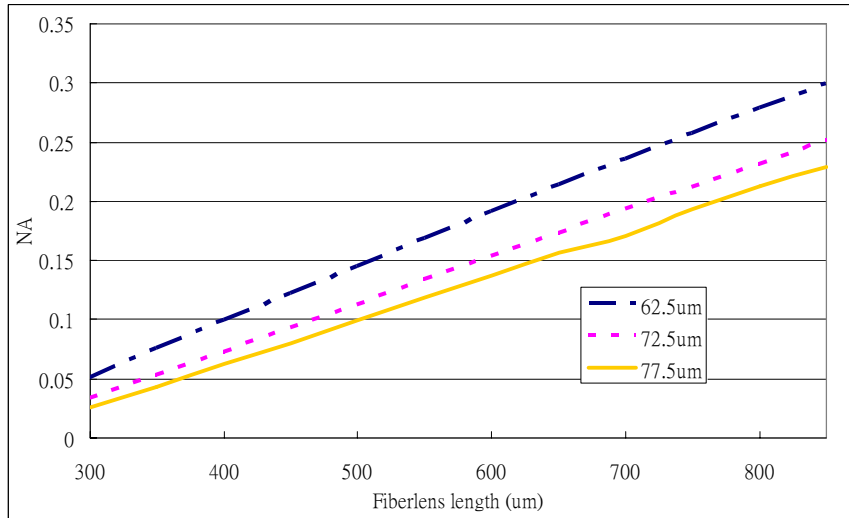
Then spot size, NA and efficiency as functions of axial, lateral and angular tolerances were also calculated and presented in next section. These results can provide information in fabrication.



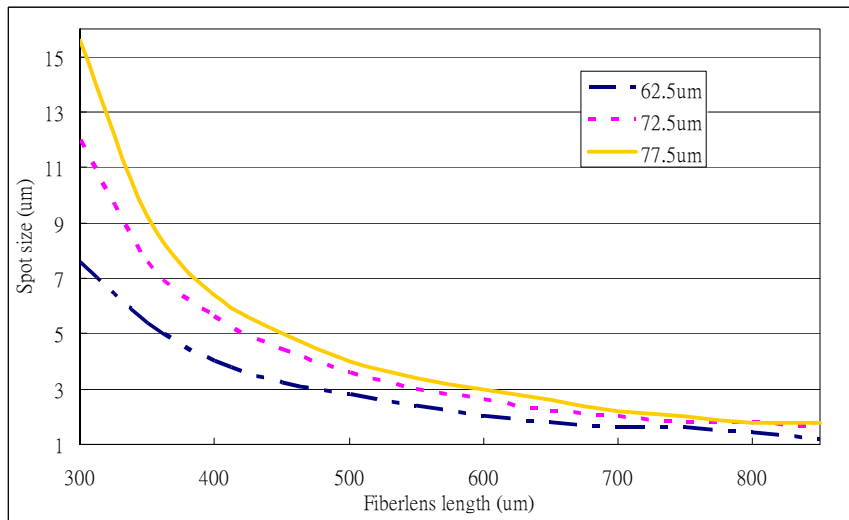
3.3.1 Radius of Fiberlens

Because the shape of fiberlens is formed by fusion splicer, the radius is difficult to control accurately. Therefore, the tolerance of the fiberlens radius is computed by using fiberlens model in Fig.3-4. The NA decreases and spot size increases with the increase of the radius of fiberlens. The relation between beam quality and radius of fiberlens is shown in Fig.3-13.

We adjust the radius based on our optimized structure. The relation between radius of fiberlens and beam quality is shown in Fig.3-14. As radius of fiberlens increases, the effective NA decreases and the spot size increases. Due to our target, the spot size is of less than $1 \mu\text{m}$ and NA is of larger 0.6, the allowable radius of fiberlens is $64.5 \mu\text{m}$.



(a)



(b)

Fig. 3-13 Fiberlens length vs. (a) NA and (b) Spot size

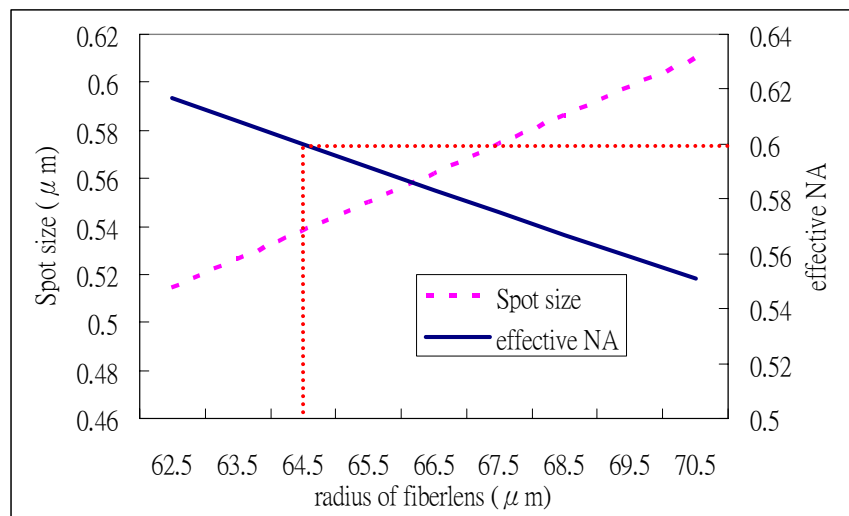


Fig. 3-14 radius of fiberlens vs. effective NA & Spot size @ 700um fiberlens

3.3.2 Thickness of SIL

The SIL is fabricated by MOEMS. The thickness of SIL is controlled by rotation speed of spinning coating and reflow process. The thickness variation caused from the fabrication is considered and defined as the variation between the optimum thickness (d_0) and real thickness (d), as shown in Fig.3-15. Under the assumption of fixing the position of SIL, the effective NA and spot size at focal plane as a function of thickness variation is shown in Fig.3-16. As the thickness varies is from $-0.5 \mu\text{m}$ to $1 \mu\text{m}$, the output beam quality is within our criteria. In MOEMS technology, the resolution which is about $1 \mu\text{m}$ is within the thickness tolerance met our design.

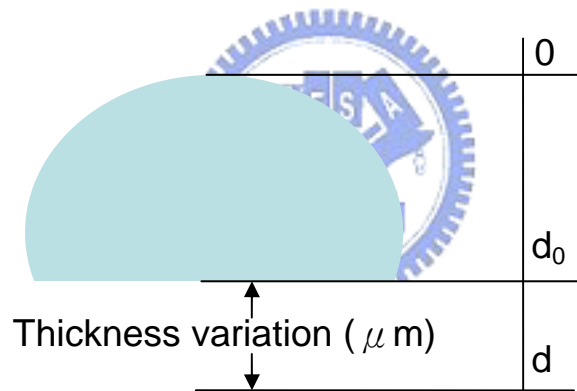


Fig. 3-15 Definition of thickness variation

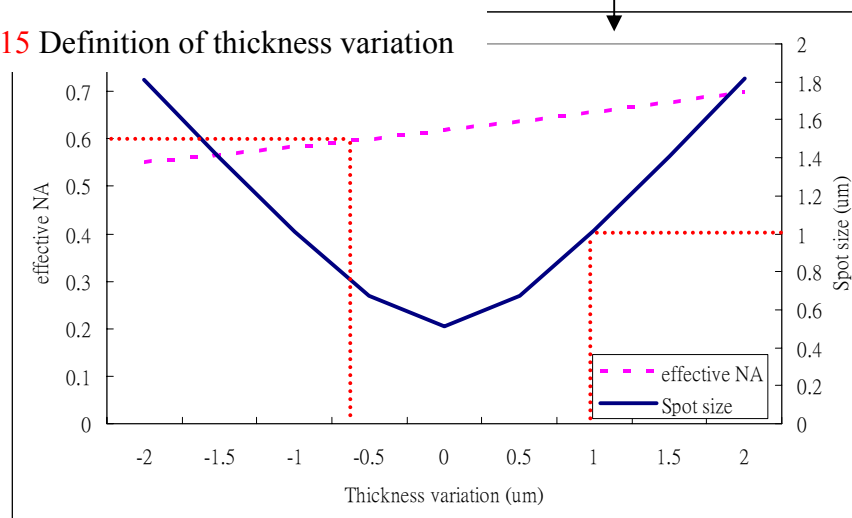


Fig. 3-16 Thickness variation of SSIL vs. effective NA & Spot size @ 700μm fiberlens

3.3.3 Alignment tolerance

Misalignments, such as axial, lateral and angular, may occur in assembly process. Three kinds of misalignments are presented in Fig.3-17.

Axial misalignment is due to the bottom of SIL is not on focal plane of fiberlens. As the distance between fiberlens and SIL is smaller than focal length, the focal plane locates on right side of SIL and spot size on bottom of SIL will increase, as shown in Fig.3-18(a), so does the NA increase. When the SIL is moved away from the fiberlens, the focal plane locates inside SIL and spot size on bottom of SIL increases while NA decreases, as shown in Fig.3-18(b). Because we expect the spot size is of less than $1 \mu\text{m}$ and NA is of larger 0.6, the allowable defocus is from $-6 \mu\text{m}$ to $3 \mu\text{m}$. The relation between defocus and beam quality is shown in Fig.3-19.

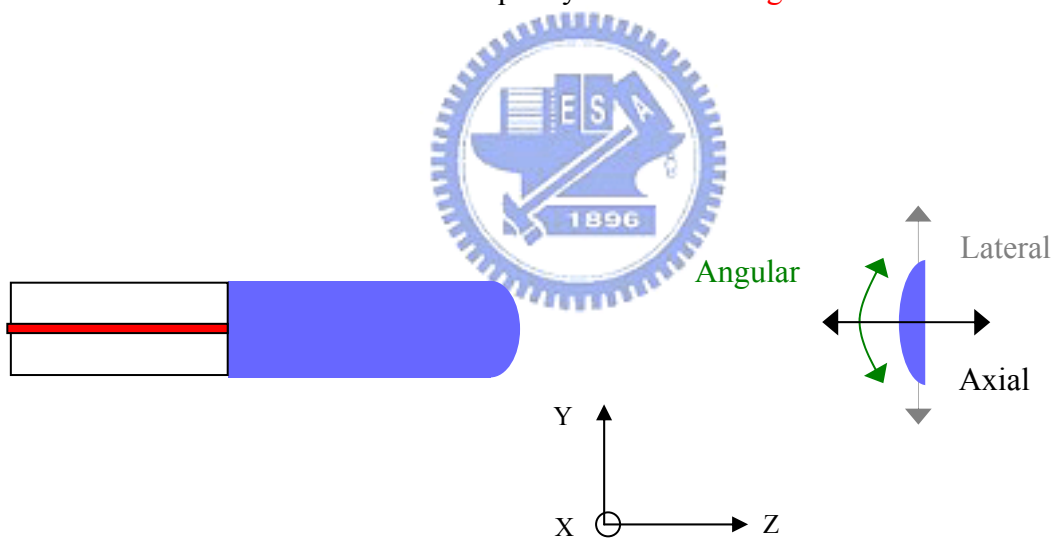


Fig. 3-17 Definition of three misalignments

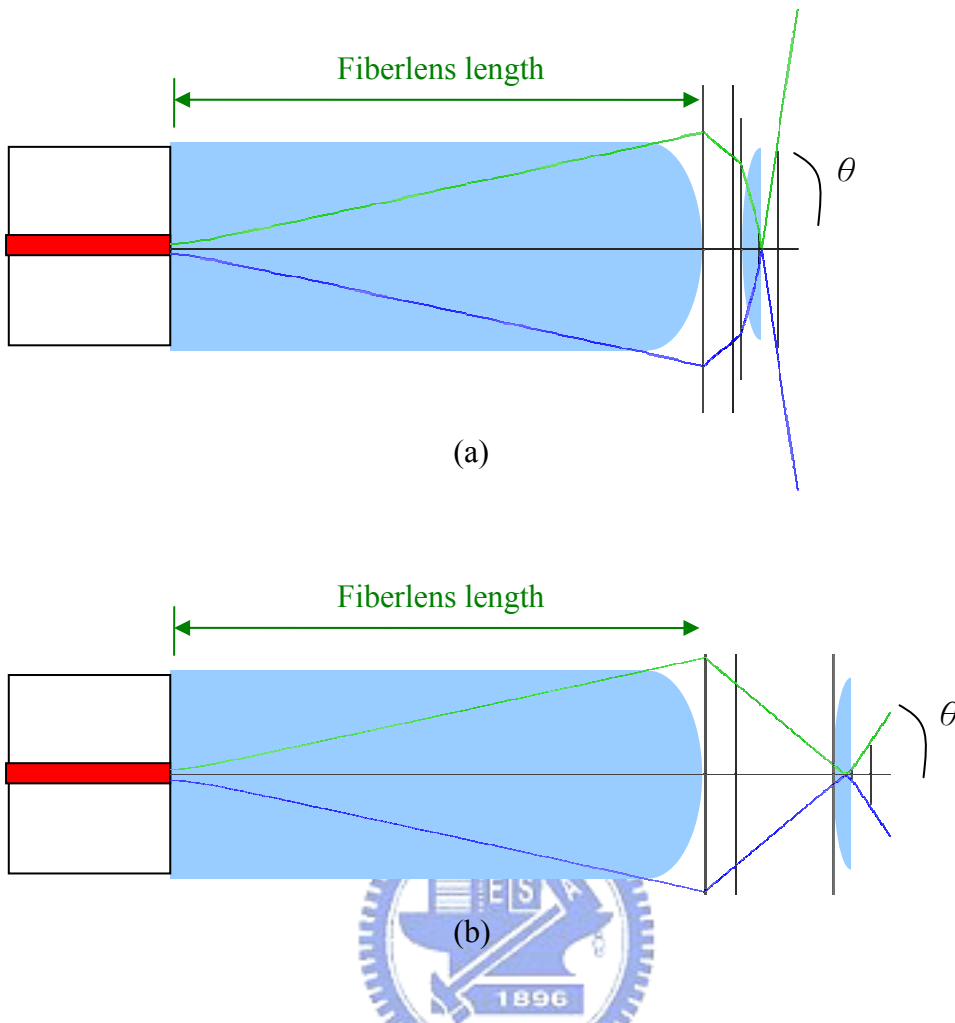


Fig. 3-18 (a) Distance between fiberlens and SIL is smaller than focal length
 (b) Distance between fiberlens and SIL is larger than focal length

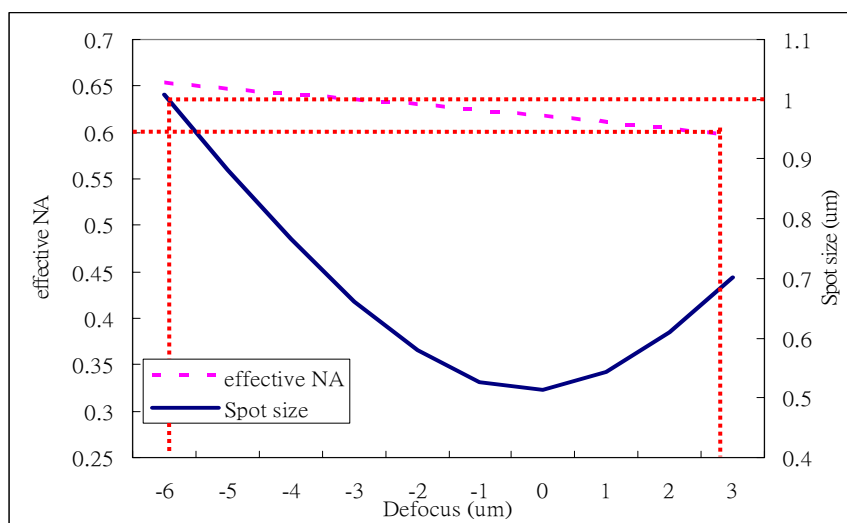


Fig. 3-19 Defocus vs. effective NA and spot size

Next, lateral misalignment is considered. Lateral misalignment causes the centric

offset due to the SIL moves on the focal plane. The spot diagrams with offset of $10\ \mu\text{m}$ along X and Y direction, and without offset are depicted in Fig.3-20. The periphery of spot is distorted and the centric shift occurs, but distribution on the central area of spot is almost the same. Here we set the aperture diameter is $1\ \mu\text{m}$ on the bottom of SIL and the criteria is that minimum efficiency is 90%. The relation between efficiency and offset are shown in Fig.3-21. As the efficiency is restricted to larger than 90%, the lateral misalignment is allowed to less than $3\ \mu\text{m}$.

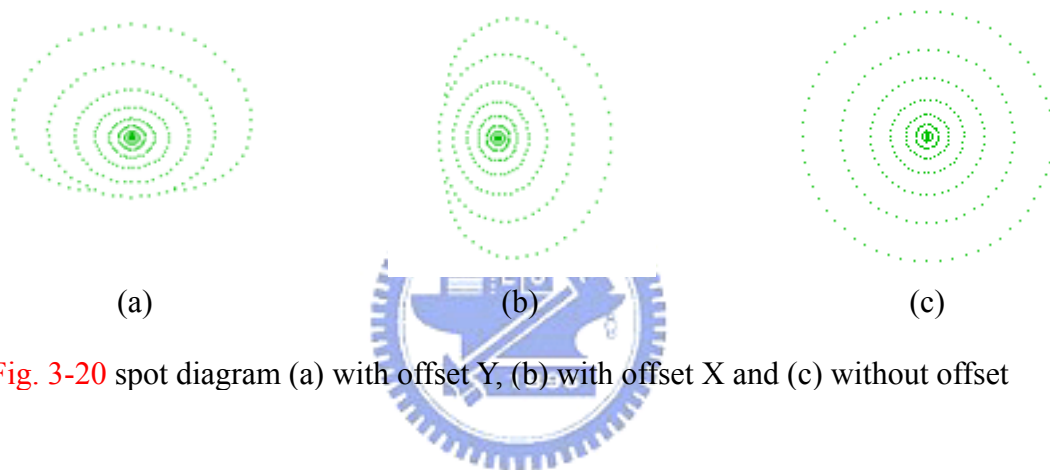


Fig. 3-20 spot diagram (a) with offset Y, (b) with offset X and (c) without offset

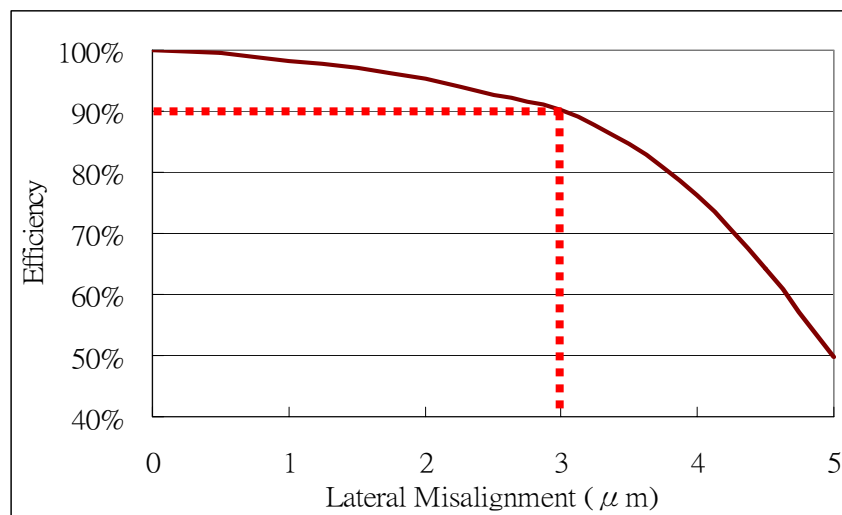


Fig. 3-21 Offset vs. Efficiency

Finally, angular misalignment is discussed. Angular misalignment causes the

centric offset due to the SIL tilt on the focal plane. The spot diagrams with tilt of 15 degree, and without tilt are simulated and result is shown in Fig.3-22. The periphery of spot is distorted and the centric shift occurs, but distribution on the central area of spot is almost the same. Angular misalignment causes the similar effect on spot as the lateral misalignment. The relation between angular misalignment and efficiency is shown in Fig.3-23. As the efficiency is larger than 90%, the angular misalignment is of less than 9 degree. The tolerance of angular misalignment is 9 degree.

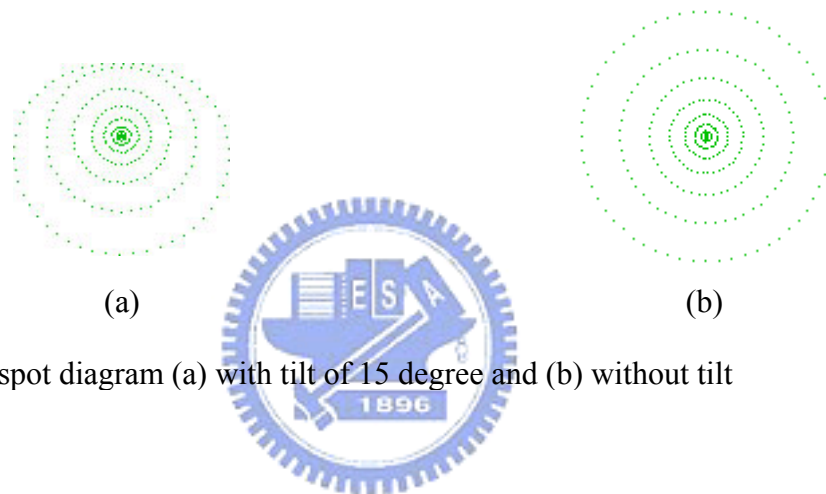


Fig. 3-22 spot diagram (a) with tilt of 15 degree and (b) without tilt

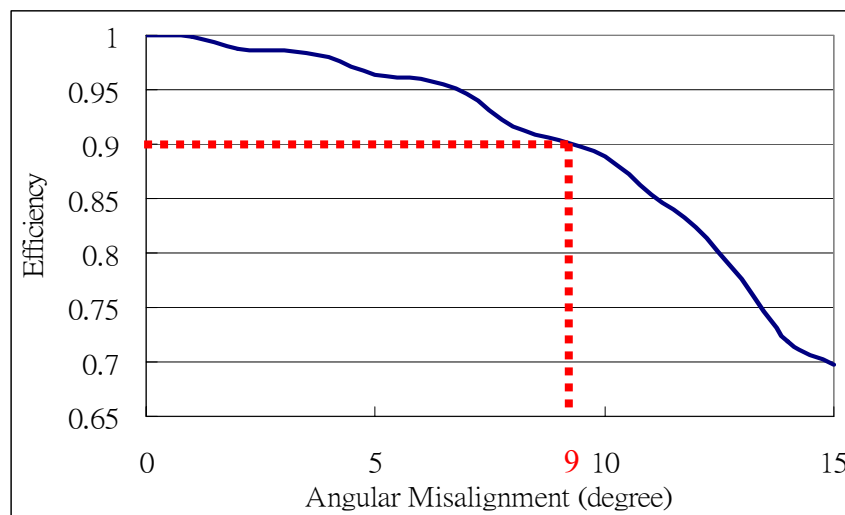


Fig. 3-23 Angular misalignment vs. Efficiency

3.4 Summary

In this module, each component was well designed based on fabrication criteria and the errors from fabrication and assembly process were discussed. The tolerance in axial misalignment is from -6 to 3 μ m, in lateral misalignment is 3 μ m and in angular misalignment is 9 degree. Positioning stage and double side alignment technology are often used in assembly process. The system tolerance is within the precision range of assembly process as shown in **Table 3-1**.

Table 3-1 Axial, Lateral & Angular Tolerance Compartment

	Axial(μ m)	Lateral(μ m)	Angular(degree)
Our Design	-6~3	3	9
Positioning stage	0.5	0.5	0.05
Double side alignment technology	1	1	0.1